A boundary integral approach for plane analysis of electrically semi-permeable planar cracks in a piezoelectric solid

W. T. Ang and L. Athanasius
Division of Engineering Mechanics
School of Mechanical and Aerospace Engineering
Nanyang Technological University
50 Nanyang Avenue
Singapore 639798

Abstract

A plane electro-elastostatic problem involving arbitrarily located planar stress free cracks which are electrically semi-permeable is considered. Through the use of the numerical Green's function for impermeable cracks, the problem is formulated in terms of boundary integral equations which are solved numerically by a boundary element procedure together with a predictor-corrector method. The crack tip stress and electric displacement intensity factors can be easily computed once the boundary integral equations are properly solved.

Keywords: boundary integral method, numerical Green's function, piezoelectric solid, electrically semi-permeable cracks.

This is a preprint of an article which has been accepted for publication in the *Engineering Analysis with Boundary Elements*. When the article is available online at the publisher, it can be accessed at the following link: http://dx.doi.org/10.1016/j.enganabound.2010.11.011

1 Introduction

In the 1970s, Snyder and Cruse [20] pioneered the approach of using special Green's functions (modified fundamental solutions) in the boundary integral method for solving crack problems. They derived an analytical Green's function for a stress free planar crack in an infinite orthotropic elastic space and applied it to analyze the stress distribution around the crack in a body of finite extent. The work in [20] was subsequently extended by other researchers to solve more complicated crack problems (see, for example, Ang [2], Ang and Clements [3] and Clements and Haselgrove [8]). The main advantage of the Green's function approach is that the singular behaviors of the stress at the crack tips are accurately captured in the boundary integral formulation of the crack problem. Furthermore, through the use of an appropriate Green's function, no integration over the crack faces is required in the boundary integral method.

In general, Green's functions for cracks with arbitrary geometries, configurations and boundary conditions are, however, difficult (if not impossible) to derive analytically. To solve a wider range of crack problems, Telles, Castor and Guimarães [18] and Guimarães and Telles [15] proposed a numerical hypersingular integral approach for deriving the required Green's function. Such a numerical Green's function approach was also used by Ang and Telles [4] to solve an elastostatic problem involving multiple interacting planar cracks in an anisotropic body.

Recently, Athanasius, Ang and Sridhar [5] extended the analysis in [4] to a plane electro-elastostatic crack problem, deriving numerical Green's functions for arbitrarily located stress free planar cracks which are either electrically impermeable or permeable. In the present paper, the numerical Green's function for the impermeable cracks is used to obtain boundary integral equations for multiple stress free electrically semi-permeable cracks. Because of the electrically semi-permeable conditions on the cracks, the boundary integral equations contain integrals whose integrands are given by a nonlinear function of the crack opening displacement and the electrical potential jump on the cracks. The boundary integral equations can be solved by using a simple numerical procedure if the crack opening displacement and the electric potential jump are known. Those physical quantities on the cracks are, however, not known a priori. A predictor-corrector approach which iterates to and fro estimating the crack opening displacement and the electrical potential jump and solving the boundary integral equations is presented here for the numerical solution of the semi-permeable crack problem.

A brief review of existing boundary integral approaches for solving piezoelectric crack problems may be appropriate at this juncture. Analytical closed form Green's functions which can be used to derive boundary element solutions for a single stress free planar crack which is either impermeable or conducting (permeable) are given in Rajapakse and Xu [17]. Garcia-Sanchez, Saez and Dominguez [12] and Groh and Kuna [13] presented numerical procedures based on boundary integral equations derived by using fundamental solution which does not satisfy the boundary conditions on the crack faces. In [13], opposite crack faces were modeled by using the so called subdomain technique and quarter-point elements were employed to deal with the singular behaviors of the stress and electric displacement at the crack tips, while a dual (mixed) boundary integral formulation was used in [12] with the conditions on the cracks treated by a differentiated form of the usual boundary integral equations. Some earlier works on boundary element methods for electroelastic crack problems include Ding, Wang and Chen [10], Gao and Fan [11], Pan [16] and Xu and Rajapakse [19]. The boundary element solutions in the references above are mostly for impermeable and conducting cracks. It appears that the only boundary element treatment of the semi-permeable crack problem is given in Denda [9]. In [9], the whole crack singular element is employed together with an iterative scheme to treat a single semi-permeable crack in a piezoelectric solid. The iterative procedure is different from the one adopted in the present paper.

2 The problem

With reference to a Cartesian co-ordinate frame denoted by $Ox_1x_2x_3$, consider a homogeneous piezoelectric solid whose geometry does not vary along the x_3 axis. The interior of the solid contains M arbitrarily located planar cracks. The exterior boundary of the solid is denoted by B and the k-th crack by $\gamma^{(k)}$. The cracks do not intersect with one another or the exterior boundary B. On the Ox_1x_2 plane, the boundary B appears as a simple closed curve and the crack $\gamma^{(k)}$ as a straight cut with tips $(a^{(k)}, b^{(k)})$ and $(c^{(k)}, d^{(k)})$. For our purpose of the analysis in the present paper, $\gamma^{(k)}$ may be regarded as a straight line segment between $(a^{(k)}, b^{(k)})$ and $(c^{(k)}, d^{(k)})$.

Either the displacements or the tractions and either the electric potential or the normal electric displacement are prescribed at each and every point on B. The prescribed conditions on B are independent of the spatial coordinate x_3 and time t. The cracks are assumed to open up and become stress free under the prescribed boundary conditions. They are also assumed to be electrically semi-permeable. Mathematically, the stress free conditions on the cracks are given by

$$\sigma_{ij}(x_1, x_2)m_j^{(k)} \to 0 \text{ as } (x_1, x_2) \to (y_1, y_2) \in \gamma^{(k)} \text{ for } k = 1, 2, \cdots, M, \quad (1)$$

and the electrical conditions for semi-permeable cracks as proposed in Hao and Shen [14] are given by

$$\begin{aligned} D_j(x_1, x_2)m_j^{(k)}\Delta u_p(x_1, x_2)m_p^{(k)} &= -\epsilon_{\mathrm{c}}\Delta\phi(x_1, x_2) \\ &\text{for } (x_1, x_2) \in \gamma^{(k)} \text{ for } k = 1, 2, \cdots, M, \end{aligned} \quad (2)$$

where ϵ_{c} is the permittivity of the medium filling the cracks, σ_{ij} and D_i are respectively the stresses and the electric displacements, $[m_1^{(k)}, m_2^{(k)}, m_3^{(k)}] = [(d^{(k)} - b^{(k)})/\ell^{(k)}, (a^{(k)} - c^{(k)})/\ell^{(k)}, 0]$ is a unit normal vector to the crack $\gamma^{(k)}$, $\ell^{(k)}$ is the length of $\gamma^{(k)}$ (that is, $\ell^{(k)} = \sqrt{(d^{(k)} - b^{(k)})^2 + (a^{(k)} - c^{(k)})^2}$), $\Delta\phi$ is the jump in the electric potential ϕ across opposite crack faces as defined by

$$\begin{aligned} \Delta\phi(x_1, x_2) = \lim_{\epsilon\to 0}[&\phi(x_1 - |\epsilon|m_1^{(k)}, x_2 - |\epsilon|m_2^{(k)}) \\ &- \phi(x_1 + |\epsilon|m_1^{(k)}, x_2 + |\epsilon|m_2^{(k)})] \\ &\text{for } (x_1, x_2) \in \gamma^{(k)}, \end{aligned} \quad (3)$$

and Δu_p is the jump in the displacement u_p across opposite crack faces, that is,

$$\begin{aligned} \Delta u_p(x_1, x_2) = \lim_{\varepsilon\to 0}[&u_p(x_1 - |\epsilon|m_1^{(k)}, x_2 - |\epsilon|m_2^{(k)}) \\ &- u_p(x_1 + |\epsilon|m_1^{(k)}, x_2 + |\epsilon|m_2^{(k)})] \\ &\text{for } (x_1, x_2) \in \gamma^{(k)}. \end{aligned} \quad (4)$$

The usual Einsteinian convention of summing over a repeated index applies here for Latin subscripts running from 1 to 3.

The problem is to determine the displacements u_k and the electric potential ϕ throughout the cracked piezoelectric solid.

3 Equations of electroelasticity

The governing partial differential equations for the displacements u_k and the electric potential ϕ in the piezoelectric solid are given by

$$\begin{aligned} c_{ijkp}\frac{\partial^2 u_k}{\partial x_j \partial x_p} + e_{pij}\frac{\partial^2 \phi}{\partial x_j \partial x_p} &= 0, \\ e_{jkp}\frac{\partial^2 u_k}{\partial x_j \partial x_p} - \kappa_{jp}\frac{\partial^2 \phi}{\partial x_j \partial x_p} &= 0, \end{aligned} \tag{5}$$

where c_{ijkp}, e_{pij} and κ_{jp} are the constant elastic moduli, piezoelectric coefficients and dielectric coefficients respectively.

The constitutive equations relating (σ_{ij}, D_j) and (u_k, ϕ) are

$$\begin{aligned} \sigma_{ij} &= c_{ijkp}\frac{\partial u_k}{\partial x_p} + e_{pij}\frac{\partial \phi}{\partial x_p}, \\ D_j &= e_{jkp}\frac{\partial u_k}{\partial x_p} - \kappa_{jp}\frac{\partial \phi}{\partial x_p}. \end{aligned} \tag{6}$$

Following closely the approach of Barnett and Lothe [6], one may let

$$U_J = \begin{cases} u_j & \text{for } J = j = 1, 2, 3, \\ \phi & \text{for } J = 4, \end{cases}$$

$$S_{Ij} = \begin{cases} \sigma_{ij} & \text{for } I = i = 1, 2, 3, \\ D_j & \text{for } I = 4, \end{cases}$$

$$C_{IjKp} = \begin{cases} c_{ijkp} & \text{for } I = i = 1, 2, 3 \text{ and } K = k = 1, 2, 3, \\ e_{pij} & \text{for } I = i = 1, 2, 3 \text{ and } K = 4, \\ e_{jkp} & \text{for } I = 4 \text{ and } K = k = 1, 2, 3, \\ -\kappa_{jp} & \text{for } I = 4 \text{ and } K = 4, \end{cases} \tag{7}$$

so that (5) and (6) may be written more compactly as

$$C_{IjKp}\frac{\partial^2 U_K}{\partial x_j \partial x_p} = 0 \tag{8}$$

and

$$S_{Ij} = C_{IjKp}\frac{\partial U_K}{\partial x_p} \tag{9}$$

respectively. Note that the uppercase Latin subscripts have values 1, 2, 3 and 4. Summation is also implied for repeated uppercase Latin subscripts running from 1 to 4.

The general solution of (8) can be written as

$$U_K(x_1, x_2) = \mathrm{Re}\{\sum_{\alpha=1}^{4} A_{K\alpha} f_\alpha(z_\alpha)\}, \tag{10}$$

where Re denotes the real part of a complex number, f_α are analytic functions of $z_\alpha = x_1 + \tau_\alpha x_2$ in the domain of interest, τ_α are the solutions, with positive imaginary parts, of the 8-th order polynomial (characteristic) equation

$$\det[C_{I1K1} + (C_{I1K2} + C_{I2K1})\tau + C_{I2K2}\tau^2] = 0 \tag{11}$$

and $A_{K\alpha}$ are solutions of the homogeneous system

$$[C_{I1K1} + (C_{I1K2} + C_{I2K1})\tau_\alpha + C_{I2K2}\tau_\alpha^2]A_{K\alpha} = 0. \tag{12}$$

Physical constraints on C_{IjKp} ensures that the characteristic equation (11) admits solutions which occur in complex conjugate pairs (Barnett and Lothe [6]). It is assumed that we can find τ_1, τ_2, τ_3 and τ_4 such that an invertible 4×4 matrix $[A_{K\alpha}]$ can be constructed from (12). For a certain degenerate case in which the deformation of the material is isotropic, it may not be possible to construct $[A_{K\alpha}]$ which is invertible. For such a case, a very small perturbation may be introduced into the elastic constants of the material to construct invertible $[A_{K\alpha}]$ (as shown in Athanasius, Ang and Sridhar [5]).

The generalized stress functions S_{Ij} corresponding to (10) are given by

$$S_{Ij} = \mathrm{Re}\{\sum_{\alpha=1}^{4} L_{Ij\alpha} f'_\alpha(z_\alpha)\}, \tag{13}$$

where the prime denotes differentiation with respect to the relevant argument and

$$L_{Ij\alpha} = (C_{IjK1} + \tau_\alpha C_{IjK2})A_{K\alpha}. \tag{14}$$

4 Boundary integral equations and numerical Green's function

If the generalized elliptic system in (5) holds in a two-dimensional region R with boundary ∂R then

$$\begin{aligned}\lambda(\xi_1,\xi_2)U_K(\xi_1,\xi_2) = \int_{\partial R} &[U_I(x_1,x_2)\Gamma_{IK}(x_1,x_2;\xi_1,\xi_2) \\ &- P_I(x_1,x_2)\Phi_{IK}(x_1,x_2;\xi_1,\xi_2)]ds(x_1,x_2),\end{aligned} \tag{15}$$

where $\lambda(\xi_1,\xi_2) = 1$ if (ξ_1,ξ_2) lies in the interior of R and $\lambda(\xi_1,\xi_2) = 1/2$ if (ξ_1,ξ_2) lies on a smooth part of ∂R, $P_I(x_1,x_2) = S_{Ij}(x_1,x_2)n_j(x_1,x_2)$, n_j is the x_j component of the unit normal outward vector to the boundary ∂R, the functions $\Phi_{RS}(x_1,x_2;\xi_1,\xi_2)$ and $\Gamma_{IK}(x_1,x_2;\xi_1,\xi_2)$ are given by

$$\begin{aligned}\Phi_{RS}(x_1,x_2;\xi_1,\xi_2) &= \Phi^{[1]}_{RS}(x_1,x_2;\xi_1,\xi_2) + \Phi^{[2]}_{RS}(x_1,x_2;\xi_1,\xi_2), \\ \Phi^{[1]}_{RS}(x_1,x_2;\xi_1,\xi_2) &= \frac{1}{2\pi}\,\mathrm{Re}\sum_{\alpha=1}^{4}\{A_{R\alpha}N_{\alpha J}\ln([x_1-\xi_1]+\tau_\alpha[x_2-\xi_2])\}\,d_{JS}, \\ \Gamma_{IK}(x_1,x_2;\xi_1,\xi_2) &= C_{IjRs}n_j(x_1,x_2)\frac{\partial}{\partial x_s}[\Phi_{RK}(x_1,x_2,\xi_1,\xi_2)],\end{aligned} \tag{16}$$

the matrix $[N_{\alpha J}]$ is the inverse of $[A_{K\alpha}]$, d_{JS} are real constants defined by

$$\mathrm{Im}\{\sum_{\alpha=1}^{4} L_{I2\alpha} N_{\alpha R}\} d_{RJ} = \delta_{IJ}, \tag{17}$$

δ_{IJ} is the Kronecker-delta and $\Phi^{[2]}_{RS}(x_1, x_2; \xi_1, \xi_2)$ is any function such that

$$c_{IjKp} \frac{\partial^2 \Phi^{[2]}_{KS}}{\partial x_j \partial x_p} = 0 \text{ for } (x_1, x_2) \text{ in } R \cup \partial R. \tag{18}$$

Note that Im denotes the imaginary part of a complex number. For details on the derivation of (15), refer to Clements [7].

For the problem stated in Section 2, the boundary consists of the outer boundary B and the faces of the cracks $\gamma^{(1)}, \gamma^{(2)}, \cdots, \gamma^{(M-1)}$ and $\gamma^{(M)}$. Thus, the boundary integral equations in (15) may be rewritten as

$$\begin{aligned}\lambda(\xi_1, \xi_2) U_K(\xi_1, \xi_2) \;=\; & \int_B [U_I(x_1, x_2)\Gamma_{IK}(x_1, x_2; \xi_1, \xi_2) \\ & - P_I(x_1, x_2)\Phi_{IK}(x_1, x_2; \xi_1, \xi_2)] ds(x_1, x_2) \\ & + \sum_{k=1}^{M} \int_{\gamma_+^{(k)}} [\Delta U_I(x_1, x_2)\Gamma_{IK}(x_1, x_2; \xi_1, \xi_2) \\ & - P_I(x_1, x_2)\Delta\Phi_{IK}(x_1, x_2; \xi_1, \xi_2)] ds(x_1, x_2),\end{aligned} \tag{19}$$

where $\Delta U_I(x_1, x_2)$ is the jump in the generalized displacements across opposite crack faces defined in (3) and (4), $\gamma_+^{(k)}$ (the "upper face" of the crack $\gamma^{(k)}$) is taken to be the straight line from $(a^{(k)}, b^{(k)})$ to $(c^{(k)}, d^{(k)})$ and

$$\begin{aligned}\Delta\Phi_{IK}(x_1, x_2; \xi_1, \xi_2) = & \lim_{\epsilon \to 0} [\Phi_{IK}(x_1 - |\epsilon| m_1^{(k)}, x_2 - |\epsilon| m_2^{(k)}; \xi_1, \xi_2) \\ & - \Phi_{IK}(x_1 + |\epsilon| m_1^{(k)}, x_2 + |\epsilon| m_2^{(k)}; \xi_1, \xi_2)] \\ & \text{for } (x_1, x_2) \in \gamma^{(k)}.\end{aligned} \tag{20}$$

Now if the Green's function $\Phi_{IK}(x_1, x_2; \xi_1, \xi_2)$ is chosen such that

$$\Gamma_{IK}(x_1, x_2; \xi_1, \xi_2) = 0 \text{ for } (x_1, x_2) \in \gamma^{(k)}, \tag{21}$$

then (20) together with (1) and (2) gives

$$\begin{aligned}\lambda(\xi_1,\xi_2)U_K(\xi_1,\xi_2) &= \int_B [U_I(x_1,x_2)\Gamma_{IK}(x_1,x_2;\xi_1,\xi_2) \\ &\quad -P_I(x_1,x_2)\Phi_{IK}(x_1,x_2;\xi_1,\xi_2)]ds(x_1,x_2) \\ &\quad -\frac{1}{2}\sum_{n=1}^{M}\ell^{(n)}\int_{-1}^{1} D^{(n)}(t)\Delta\Phi_{4K}^{(n)}(t;\xi_1,\xi_2)dt, \quad (22)\end{aligned}$$

where $\Delta\Phi_{4K}^{(n)}(t;\xi_1,\xi_2) = \Delta\Phi_{4K}(X_1^{(n)}(t),X_2^{(n)}(t);\xi_1,\xi_2)$, $2X_1^{(n)}(t) = [c^{(n)} + a^{(n)}] + [c^{(n)} - a^{(n)}]t, 2X_2^{(n)}(t) = [d^{(n)} + b^{(n)}] + [d^{(n)} - b^{(n)}]t$ and

$$D^{(n)}(t) = -\frac{\epsilon_{\mathrm{c}}\Delta U_4(X_1^{(n)}(t),X_2^{(n)}(t))}{\Delta U_1(X_1^{(n)}(t),X_2^{(n)}(t))m_1^{(n)} + \Delta U_2(X_1^{(n)}(t),X_2^{(n)}(t))m_2^{(n)}}. \quad (23)$$

The function $\Phi_{RS}^{[2]}(x_1,x_2;\xi_1,\xi_2)$ chosen to satisfy (21) can be constructed numerically as explained in Athanasius, Ang and Sridhar [5]. Specifically, $\Phi_{RS}^{[2]}(x_1,x_2;\xi_1,\xi_2)$ is approximately given by

$$\begin{aligned}\Phi_{RS}^{[2]}(x_1,x_2;\xi_1,\xi_2) &= \frac{1}{2}\sum_{n=1}^{M}\ell^{(n)}\int_{-1}^{1}\Delta\Phi_{PS}^{(n)}(t;\xi_1,\xi_2) \\ &\quad \times\Lambda_{PR}^{(n)}(x_1,x_2;X_1^{(n)}(t),X_2^{(n)}(t))dt, \\ \Delta\Phi_{PS}^{(n)}(t;\xi_1,\xi_2) &= \Delta\Phi_{PS}(X_1^{(n)}(t),X_2^{(n)}(t);\xi_1,\xi_2) \\ &\simeq \sqrt{1-t^2}\sum_{j=1}^{J}\phi_{PS}^{(nj)}(\xi_1,\xi_2)U^{(j-1)}(t), \quad (24)\end{aligned}$$

where $\Lambda_{IS}^{(n)}(x_1,x_2;y_1,y_2)$ is defined by

$$\Lambda_{IS}^{(n)}(x_1,x_2;y_1,y_2) = -\frac{1}{2\pi}\,\mathrm{Re}\sum_{\alpha=1}^{4}\{\frac{T_{Ij\alpha S}m_j^{(n)}}{[x_1-y_1]+\tau_\alpha[x_2-y_2]}\}, \quad (25)$$

$T_{Ij\alpha S} = L_{Ij\alpha}N_{\alpha R}d_{RS}$, $U^{(j)}(x) = \sin([j+1]\arccos(x))/\sin(\arccos(x))$ $(-1 < x < 1)$ is the j-th order Chebyshev polynomial of the second kind and

$\phi_{PS}^{(nj)}(\xi_1, \xi_2)$ are determined by solving the system

$$
\begin{aligned}
&-\sum_{j=1}^{J} j\pi\phi_{PS}^{(qj)}(\xi_1,\xi_2)\chi_{PK}^{(q)}U^{(j-1)}(t^{(i)}) \\
&+\sum_{j=1}^{J}\sum_{\substack{n=1\\ n\neq q}}^{M}\phi_{PS}^{(nj)}(\xi_1,\xi_2)\int_{-1}^{1}\sqrt{1-v^2}U^{(j-1)}(v)Y_{PK}^{(nq)}(v,t^{(i)})dv \\
&=\Lambda_{KS}^{(q)}(X_1^{(q)}(t^{(i)}), X_2^{(q)}(t^{(i)}), \xi_1, \xi_2) \\
&\text{for } i=1,2,\cdots,J,\ K=1,2,3,4,\ S=1,2,3,4 \text{ and } q=1,2,\cdots,M, \qquad (26)
\end{aligned}
$$

where $t^{(i)} = \cos([2i-1]\pi/[2J])$, $\chi_{PK}^{(q)}$ and $Y_{PK}^{(nq)}(v,t)$ are defined by

$$
\begin{aligned}
\chi_{PK}^{(q)} &= \frac{1}{\pi}\,\mathrm{Re}\sum_{\alpha=1}^{4}\{\frac{\ell^{(q)}Q_{PKrj\alpha}m_r^{(q)}m_j^{(q)}}{[(c^{(q)}-a^{(q)})+\tau_\alpha(d^{(q)}-b^{(q)})]^2}\}, \\
Y_{PK}^{(nq)}(v,t) &= \frac{1}{4\pi}\,\mathrm{Re}\sum_{\alpha=1}^{4}\{\frac{\ell^{(n)}Q_{PKrj\alpha}m_r^{(q)}m_j^{(n)}}{[\Xi^{(nq)}(v,t)+\tau_\alpha\Theta^{(nq)}(v,t)]^2}\}, \qquad (27)
\end{aligned}
$$

with $\Xi^{(nq)}(v,t) = X_1^{(n)}(v) - X_1^{(q)}(t)$, $\Theta^{(nq)}(v,t) = X_2^{(n)}(v) - X_2^{(q)}(t)$ and $Q_{PKrj\alpha} = (C_{KrI1} + \tau_\alpha C_{KrI2})T_{Pj\alpha I}$.

5 Numerical procedure

A numerical method based on the boundary integral equations in (22) together with the Green's function defined by (16) and (24) is given below for solving the crack problem stated in Section 2.

5.1 Boundary elements

From the given boundary conditions on the exterior boundary B, either $U_I = u_i$ or $P_I = p_i$ for $I = i = 1,2,3$, and either $U_4 = \phi$ or P_4 are known at each and every point on B. If $D^{(n)}(t)$ is assumed known, the boundary B and the integral equations (22) can be discretized to determine approximately the unknown generalized displacements U_I and/or tractions P_I on B. To do this, the boundary B is approximated using N straight line segments denoted by $B^{(1)}$, $B^{(2)}$, $\cdots$, $B^{(N-1)}$ and $B^{(N)}$. Across the segment $B^{(m)}$, the displacements U_I and the tractions P_I are approximated by constants $U_I^{(m)}$ and $P_I^{(m)}$ respectively. Through approximating (22), the unknown constants on the boundary elements $U_I^{(m)}$ and/or tractions $P_I^{(m)}$ can be determined from the system of linear algebraic equations

$$\begin{aligned}\frac{1}{2}U_K^{(m)} &= \sum_{n=1}^{N} U_I^{(n)} \int_{B^{(n)}} \Gamma_{IK}(x_1, x_2; \xi_1^{(m)}, \xi_2^{(m)}) ds(x_1, x_2) \\ &- \sum_{n=1}^{N} P_I^{(n)} \int_{B^{(n)}} \Phi_{IK}(x_1, x_2; \xi_1^{(m)}, \xi_2^{(m)}) ds(x_1, x_2) \\ &- \frac{1}{2}\sum_{n=1}^{M} \ell^{(n)} \int_{-1}^{1} D^{(n)}(t) \Delta\Phi_{4K}^{(n)}(t; \xi_1^{(m)}, \xi_2^{(m)}) dt \\ &\qquad\qquad \text{for } m = 1, 2, \cdots , N,\end{aligned} \tag{28}$$

where $(\xi_1^{(m)}, \xi_2^{(m)})$ is the midpoint of $B^{(m)}$.

From (24), the last integral in (28) can be approximated as

$$\begin{aligned}&\int_{-1}^{1} D^{(n)}(t)\Delta\Phi_{4K}^{(n)}(t; \xi_1^{(m)}, \xi_2^{(m)}) dt \\ \simeq \; &\sum_{j=1}^{J} \phi_{4S}^{(nj)}(\xi_1^{(m)}, \xi_2^{(m)}) \int_{-1}^{1} \sqrt{1-t^2}\, U^{(j-1)}(t) D^{(n)}(t) dt.\end{aligned} \tag{29}$$

The integral whose integrand is given by $\sqrt{1-t^2}U^{(j-1)}(t)D^{(n)}(t)$ can be easily and accurately computed by using the numerical quadrature formula (25.4.40) listed in Abramowitz and Stegun [1] if the function $D^{(n)}(t)$ is known.

5.2 Generalized crack opening displacements

Once $U_I^{(m)}$ and $P_I^{(m)}$ are all known, the generalized crack opening displacements on the crack $\gamma^{(n)}$, that is, $\Delta U_P^{(n)}(t) = \Delta U_P(X_1^{(n)}(t), X_2^{(n)}(t))$ for $-1 < t < 1$, can be computed numerically. Specifically, $\Delta U_P^{(n)}(t)$ is given approximately by

$$\Delta U_P^{(n)}(t) \simeq \sqrt{1-t^2}\sum_{j=1}^{J} \psi_P^{(nj)} U^{(j-1)}(t), \tag{30}$$

where the constants $\psi_P^{(nj)}$ are determined by the system of linear algebaic equations

$$\begin{aligned} & -\sum_{j=1}^{J} j\pi\psi_P^{(qj)}\chi_{PK}^{(q)}U^{(j-1)}(t^{(i)}) \\ & +\sum_{j=1}^{J}\sum_{\substack{n=1 \\ n\neq q}}^{M}\psi_P^{(nj)}\int_{-1}^{1}\sqrt{1-v^2}U^{(j-1)}(v)Y_{PK}^{(nq)}(v,t^{(i)})dv \\ = \; & S_K^{(q)}(t^{(i)}) \text{ for } i=1,2,\cdots,J,\ K=1,2,3,4 \text{ and } q=1,2,\cdots,M, \end{aligned} \tag{31}$$

where $t^{(i)} = \cos([2i-1]\pi/[2J])$ as in (26) and $S_K^{(q)}(t)$ is given by

$$\begin{aligned} S_K^{(q)}(t) = & \sum_{n=1}^{N} C_{KjRs}m_j^{(q)}\int_{B^{(n)}}\{P_I^{(n)}\frac{\partial}{\partial\xi_s}[\Phi_{IR}^{[1]}(x_1,x_2,\xi_1,\xi_2)]\Big|_{(\xi_1,\xi_2)=(X_1^{(q)}(t),X_2^{(q)}(t))} \\ & - U_I^{(n)}\frac{\partial}{\partial\xi_s}[\Gamma_{IR}^{[1]}(x_1,x_2,\xi_1,\xi_2)]\Big|_{(\xi_1,\xi_2)=(X_1^{(q)}(t),X_2^{(q)}(t))}\}ds(x_1,x_2) \\ & + \delta_{K4}D^{(q)}(t). \end{aligned} \tag{32}$$

For an idea on how (30), (31) and (32) may be obtained, one may refer to Athanasius, Ang and Sridhar [5].

5.3 Iterative solution

From (23), the function $D^{(n)}(t)$ is given by an expression which is a nonlinear function of the generalized crack opening displacements $\Delta U_1^{(n)}(t)$, $\Delta U_2^{(n)}(t)$ and $\Delta U_4^{(n)}(t)$. Thus, it is an unknown function to be determined in the process of solving the crack problem under consideration. An iterative procedure for solving the problem is given in the steps below.

1. Make a guess of $D^{(n)}(t)$. If a solution of the problem for some value of ϵ_c which is close to the desired permittivity of the medium filling the cracks is known, it can be used to provide an initial estimate of $D^{(n)}(t)$ through the formula (23). For a cold start, $D^{(n)}(t) = 0$ which corresponds to the case of impermeable cracks may be used. Go to Step 2.

2. Solve (28) for the unknown generalized displacements U_I and/or tractions P_I on the exterior boundary B using the latest estimate of $D^{(n)}(t)$. Go to Step 3.

3. Solve (31) for $\psi_P^{(qj)}$ using the latest values of $U_I^{(n)}$ and $P_I^{(n)}$and use (23) and (30) to obtain a new estimate of $D^{(n)}(t)$, that is,

$$D^{(n)}(t) = -\epsilon_c\{\sum_{j=1}^{J}\psi_4^{(nj)}U^{(j-1)}(t)\}[\sum_{p=1}^{2}\sum_{j=1}^{J}\psi_p^{(nj)}U^{(j-1)}(t)m_p^{(n)}]^{-1}. \quad (33)$$

   Check whether the newly obtained values $D^{(n)}(t^{(i)})$ ($t^{(i)} = \cos([2i - 1]\pi/[2J])$ for $i = 1, 2, \cdots, J$) agree with the previous values to within a specified number of significant figures. If the required convergence is not achieved, go back to Step 2.

In Step 2, (28) gives a system of $4N$ linear algebraic equations in $4N$ unknowns, that is, it can be written in the matrix form $\mathbf{AX} = \mathbf{B}$, where $\mathbf{A}$ and $\mathbf{B}$ are respectively known $4N \times 4N$ and $4N \times 1$ matrices and $\mathbf{X}$ is an unknown $4N \times 1$ matrix. The square matrix $\mathbf{A}$ does not change during the iterations between Steps 2 and 3. Similarly, the square matrix in the linear system of algebraic equations in (31) for determining $\psi_P^{(qj)}$ in Step 3 remains the same throughout the iterative procedure. Thus, those square matrices have to be set up and processed only once for solving the systems of linear algebraic equations.

Note that the iterative procedure proposed above differs from the one given in Denda [9] for a single semi-permeable crack. In [9], the jump in the electric potential over the impermeable crack is first obtained. This jump in electric potential is then progressively decreased to zero over the entire crack by gradually changing the value of a control parameter p. For each value of p, the solution for the corresponding permeable crack is used to compute the normal electric displacement and the generalized displacement jumps over the crack in order to estimate the permittivity ϵ_{c} which corresponds to the control parameter p. Physical quantities of interest such as the generalized stress intensity factors may then be plotted against ϵ_{c}or p. The desired solution for any other value of ϵ_{c} is finally obtained through interpolation. For each value of p, the approximation of ϵ_{c} from the solution of the permeable crack may, however, contain some errors, particularly for the case in which the crack lies in a body of finite extent, and further investigation is needed to improve the algorithm in [9].

Our iterative approach here is a more direct one. The numerical Green's function for the impermeable cracks is used in each iterative step and the iteration is between the calculation of the generalized displacements and tractions on the exterior boundary and the normal electric displacements on the cracks. As explained above, for any desired value of ϵ_c, we start with an initial guess of the normal electric displacement $D^{(n)}(t)$ and iterate until the change in $D^{(n)}(t)$ is sufficiently small. As shown in the numerical examples, convergence to the final solution may be slow for $\epsilon_c$which is relatively large. The convergence may, however, be improved significantly by replacing (33) with (45), that is, by introducing a relaxation parameter ω.

6 Generalized stress intensity factors

At the tips $(a^{(n)}, b^{(n)})$ and $(c^{(n)}, d^{(n)})$ of the n-th crack $\gamma^{(n)}$, define the stress and electric displacement intensity factors:

$$\begin{aligned} K_I(a^{(n)}, b^{(n)}) &= \lim_{t\to -1^-} \sqrt{\frac{\ell^{(n)}}{2}} \sqrt{-2(t+1)} (S_{1j}(X_1^{(n)}(t), X_2^{(n)}(t)) m_1^{(n)} \\ &\quad + S_{2j}(X_1^{(n)}(t), X_2^{(n)}(t)) m_2^{(n)}) m_j^{(n)}, \end{aligned}$$

$$\begin{aligned} K_{II}(a^{(n)}, b^{(n)}) &= \lim_{t\to -1^-} \sqrt{\frac{\ell^{(n)}}{2}} \sqrt{-2(t+1)} (S_{1j}(X_1^{(n)}(t), X_2^{(n)}(t)) m_2^{(n)} \\ &\quad - S_{2j}(X_1^{(n)}(t), X_2^{(n)}(t)) m_1^{(n)}) m_j^{(n)}, \end{aligned}$$

$$K_{III}(a^{(n)}, b^{(n)}) = \lim_{t\to -1^-} \sqrt{\frac{\ell^{(n)}}{2}} \sqrt{-2(t+1)} S_{3j}(X_1^{(n)}(t), X_2^{(n)}(t)) m_j^{(n)},$$

$$K_{IV}(a^{(n)}, b^{(n)}) = \lim_{t\to -1^-} \sqrt{\frac{\ell^{(n)}}{2}} \sqrt{-2(t+1)} S_{4j}(X_1^{(n)}(t), X_2^{(n)}(t)) m_j^{(n)},$$

$$\begin{aligned} K_I(c^{(n)}, d^{(n)}) &= \lim_{t\to 1^+} \sqrt{\frac{\ell^{(n)}}{2}} \sqrt{2(t-1)} (S_{1j}(X_1^{(n)}(t), X_2^{(n)}(t)) m_1^{(n)} \\ &\quad + S_{2j}(X_1^{(n)}(t), X_2^{(n)}(t)) m_2^{(n)}) m_j^{(n)}, \end{aligned}$$

$$
\begin{aligned}
K_{II}(c^{(n)},d^{(n)}) &= \lim_{t\to 1^+}\sqrt{\frac{\ell^{(n)}}{2}}\sqrt{2(t-1)}(S_{1j}(X_1^{(n)}(t),X_2^{(n)}(t))m_2^{(n)} \\
&\quad -S_{2j}(X_1^{(n)}(t),X_2^{(n)}(t))m_1^{(n)})m_j^{(n)},
\end{aligned}
$$

$$
K_{III}(c^{(n)},d^{(n)}) = \lim_{t\to 1^+}\sqrt{\frac{\ell^{(n)}}{2}}\sqrt{2(t-1)}S_{3j}(X_1^{(n)}(t),X_2^{(n)}(t))m_j^{(n)},
$$

$$
K_{IV}(c^{(n)},d^{(n)}) = \lim_{t\to 1^+}\sqrt{\frac{\ell^{(n)}}{2}}\sqrt{2(t-1)}S_{4j}(X_1^{(n)}(t),X_2^{(n)}(t))m_j^{(n)}. \tag{34}
$$

Once the constants $\psi_P^{(nj)}$ in (30) are determined, the generalized stress intensity factors can be computed by

$$
\begin{aligned}
K_I(a^{(n)},b^{(n)}) &\simeq \sqrt{\frac{\ell^{(n)}}{2}}\pi(\chi_{P1}^{(n)}m_1^{(n)}+\chi_{P2}^{(n)}m_2^{(n)})\sum_{j=1}^{J}\psi_P^{(nj)}U^{(j-1)}(-1), \\
K_{II}(a^{(n)},b^{(n)}) &\simeq \sqrt{\frac{\ell^{(n)}}{2}}\pi(\chi_{P1}^{(n)}m_2^{(n)}-\chi_{P2}^{(n)}m_1^{(n)})\sum_{j=1}^{J}\psi_P^{(nj)}U^{(j-1)}(-1),
\end{aligned}
$$

$$
\begin{aligned}
K_{III}(a^{(n)},b^{(n)}) &\simeq -\sqrt{\frac{\ell^{(n)}}{2}}\pi\chi_{P3}^{(n)}\sum_{j=1}^{J}\psi_P^{(nj)}U^{(j-1)}(-1), \\
K_{IV}(a^{(n)},b^{(n)}) &\simeq -\sqrt{\frac{\ell^{(n)}}{2}}\pi\chi_{P4}^{(n)}\sum_{j=1}^{J}\psi_P^{(nj)}U^{(j-1)}(-1),
\end{aligned}
$$

$$
\begin{aligned}
K_I(c^{(n)},d^{(n)}) &\simeq \sqrt{\frac{\ell^{(n)}}{2}}\pi(\chi_{P1}^{(n)}m_1^{(n)}+\chi_{P2}^{(n)}m_2^{(n)})\sum_{j=1}^{J}\psi_P^{(nj)}U^{(j-1)}(+1), \\
K_{II}(c^{(n)},d^{(n)}) &\simeq \sqrt{\frac{\ell^{(n)}}{2}}\pi(\chi_{P1}^{(n)}m_2^{(n)}-\chi_{P2}^{(n)}m_1^{(n)})\sum_{j=1}^{J}\psi_P^{(nj)}U^{(j-1)}(+1),
\end{aligned}
$$

$$
\begin{aligned}
K_{III}(c^{(n)},d^{(n)}) &\simeq -\sqrt{\frac{\ell^{(n)}}{2}}\pi\chi_{P3}^{(n)}\sum_{j=1}^{J}\psi_P^{(nj)}U^{(j-1)}(+1), \\
K_{IV}(c^{(n)},d^{(n)}) &\simeq -\sqrt{\frac{\ell^{(n)}}{2}}\pi\chi_{P4}^{(n)}\sum_{j=1}^{J}\psi_P^{(nj)}U^{(j-1)}(+1). \qquad (35)
\end{aligned}
$$

7 Specific problems

The numerical procedure in Section 5 is applied here to some specific problems involving semi-permeable cracks in piezoelectric solids.

Let us first consider a single crack $-a < x_1 < a$, $x_2 = 0$, in the square region $-h < x_1 < h$, $-h < x_2 < h$, where a and h are given positive constants. The boundary conditions on the exterior boundary B are given by

$$\begin{aligned}
P_1 &= 0 \text{ and } P_3 = 0 \text{ on } B, \\
P_2 &= \begin{cases} T_0 & \text{for } -h < x_1 < h, \ x_2 = h, \\ -T_0 & \text{for } -h < x_1 < h, \ x_2 = -h, \\ 0 & \text{for } -h < x_2 < h, \ x_1 = \pm h, \end{cases} \\
P_4 &= \begin{cases} D_0 & \text{for } -h < x_1 < h, \ x_2 = h, \\ -D_0 & \text{for } -h < x_1 < h, \ x_2 = -h, \\ 0 & \text{for } -h < x_2 < h, \ x_1 = \pm h, \end{cases}
\end{aligned}$$

where T_0 and D_0 are given positive constants.

The electrical poling direction is taken to be along the x_2 direction with the constitutive equations given by

$$\begin{aligned}
\sigma_{11} &= A\gamma_{11} + F\gamma_{22} + N\gamma_{33} - e_2 E_2, \\
\sigma_{22} &= F\gamma_{11} + C\gamma_{22} + F\gamma_{33} - e_3 E_2, \\
\sigma_{33} &= N\gamma_{11} + F\gamma_{22} + A\gamma_{33} - e_2 E_2, \\
\sigma_{32} &= 2L\gamma_{32} - e_1 E_3, \\
\sigma_{31} &= (A - N)\,\gamma_{31}, \\
\sigma_{12} &= 2L\gamma_{12} - e_1 E_1, \qquad (36)
\end{aligned}$$

and

$$
\begin{aligned}
D_1 &= 2e_1\gamma_{12} + \epsilon_1 E_1, \\
D_2 &= e_2\gamma_{11} + e_3\gamma_{22} + e_2\gamma_{33} + \epsilon_2 E_2, \\
D_3 &= 2e_1\gamma_{32} + \epsilon_1 E_3,
\end{aligned}
\tag{37}
$$

where $2\gamma_{kj} = \partial u_k/\partial x_j + \partial u_j/\partial x_k$ and $E_k = -\partial\phi/\partial x_k$. Note that $\gamma_{33} = 0$ and $E_3 = 0$ here since u_k and ϕ are independent of x_3.

It follows that the non-zero coefficients C_{IjKp} are

$$
\begin{aligned}
& C_{1111} = C_{3333} = A,\ C_{1133} = C_{3311} = N,\ C_{2222} = C, \\
& C_{1122} = C_{2211} = C_{2233} = C_{3322} = F, \\
& C_{1212} = C_{2112} = C_{2121} = C_{1221} = C_{2323} = C_{3223} = C_{3232} = C_{2332} = L, \\
& C_{1313} = C_{3113} = C_{3131} = C_{1331} = \frac{1}{2}(A-N), \\
& C_{2141} = C_{1241} = C_{3243} = C_{2343} = C_{4121} = C_{4112} = C_{4332} = C_{4323} = e_1, \\
& C_{1142} = C_{3342} = C_{4211} = C_{4233} = e_2, \\
& C_{2242} = C_{4222} = e_3,\ C_{4141} = C_{4343} = -\epsilon_1,\ C_{4242} = -\epsilon_2.
\end{aligned}
\tag{38}
$$

and the matrix $[A_{K\alpha}]$ can then be obtained by finding non-trivial solutions of the homogeneous systems

$$
\begin{aligned}
\left(A + L\tau_\alpha^2\right) A_{1\alpha} + (F+L)\,\tau_\alpha A_{2\alpha} + (e_1+e_2)\,\tau_\alpha A_{4\alpha} &= 0, \\
(F+L)\,\tau_\alpha A_{1\alpha} + \left(L + C\tau_\alpha^2\right) A_{2\alpha} + \left(e_1 + e_3\tau_\alpha^2\right) A_{4\alpha} &= 0, \\
\left(\frac{1}{2}(A-N) + L\tau_\alpha^2\right) A_{3\alpha} &= 0, \\
(e_1+e_2)\,\tau_\alpha A_{1\alpha} + \left(e_1 + e_3\tau_\alpha^2\right) A_{2\alpha} + \left(-\epsilon_1 - \epsilon_2\tau_\alpha^2\right) A_{4\alpha} &= 0,
\end{aligned}
\tag{39}
$$

where

$$
\tau_3 = i\sqrt{\frac{A-N}{2L}} \quad (A > N), \tag{40}
$$

and τ_1, τ_2 and τ_4 are solutions (with positive imaginary parts) of the sextic equation in τ given by

$$\det \begin{pmatrix} A+L\tau^2 & (F+L)\tau & (e_1+e_2)\tau \\ (F+L)\tau & L+C\tau^2 & e_1+e_3\tau^2 \\ (e_1+e_2)\tau & e_1+e_3\tau^2 & -\epsilon_1-\epsilon_2\tau^2 \end{pmatrix} = 0. \tag{41}$$

For $\alpha = 3$, a non-trivial solution of (39) which forms the third column of the matrix $[A_{K\alpha}]$ is given by

$$\begin{pmatrix} A_{13} \\ A_{23} \\ A_{33} \\ A_{43} \end{pmatrix} = \begin{pmatrix} 0 \\ 0 \\ 1 \\ 0 \end{pmatrix}. \tag{42}$$

For $\alpha = 1$, 2 and 4, if $(A+L\tau_\alpha^2)(L+C\tau_\alpha^2)-(F+L)^2\tau_\alpha^2 \neq 0$, we may take $A_{3\alpha}=0$ and $A_{4\alpha}=1$ and find $A_{1\alpha}$ and $A_{2\alpha}$ by solving

$$\begin{aligned} \left(A+L\tau_\alpha^2\right)A_{1\alpha}+(F+L)\,\tau_\alpha A_{2\alpha} &= 0, \\ (F+L)\,\tau_\alpha A_{1\alpha}+\left(L+C\tau_\alpha^2\right)A_{2\alpha} &= 0, \end{aligned} \tag{43}$$

in order to construct the first, second and fourth columns of the matrix $[A_{K\alpha}]$.

For illustrative purpose, we use the material constants of a class of PZT4 piezoceramics in our calculation, that is,

$$\begin{aligned} & A = 13.9\times 10^{10},\ N = 7.78\times 10^{10},\ F = 7.43\times 10^{10}, \\ & C = 11.3\times 10^{10},\ L = 2.56\times 10^{10}, \\ & e_1 = 13.44,\ e_2 = -6.98,\ e_3 = 13.84, \\ & \epsilon_1 = 60\times 10^{-10},\ \epsilon_2 = 54.7\times 10^{-10}. \end{aligned} \tag{44}$$

The values of A, N, F, C and L above are in N/m^2, e_1, e_2 and e_3 are in C/m^2, and ϵ_1 and ϵ_2 are in C/(Vm). The load ratio is taken to be given by $D_0/T_0 = 10^{-10}$ C/N.

Table 1. Numerical and analytical values of $K_{IV}(a,0)/(D_0\sqrt{a})$ for selected values of $\epsilon_c T_0/D_0^2$.

$\epsilon_c T_0/D_0^2$	Numerical	Analytical
0	1.00006	1.00000
0.001	1.00013	1.00007
0.01	1.00074	1.00068
0.05	1.00346	1.00339
0.1	1.00683	1.00677
0.2	1.01353	1.01346
0.5	1.03323	1.03314
1	1.06478	1.06467
5	1.27215	1.27151
10	1.45431	1.45496
20	1.69190	1.69216
50	2.02325	2.02027
∞	2.53459	2.53300

For the limiting case in which $h/a \to \infty$ (the case of a piezoelectric solid of an infinite extent), an analytical solution of the problem can be derived as shown in the Appendix, if the electric displacement D_2 can be assumed to be a constant on the crack. To check the validity of the iterative scheme proposed in Section 5 for electrically semi-permeable cracks, the numerical electric displacement intensity factor $K_{IV}(a,0)/(D_0\sqrt{a})$ (at the crack tip $(a,0)$) obtained from the iterative scheme using $h/a = 30$, 40 equal length elements and $J = 10$ (10 collocation points on the crack) are compared in Table 1 with the exact one extracted from the analytical solution in the Appendix for various values of the non-dimensionalized permittivity $\epsilon_c T_0/D_0^2$.

It is clear there is a good agreement between the numerical and analytical values of $K_{IV}(a,0)/(D_0\sqrt{a})$ in Table 1. The numerical values are obtained by gradually increasing $\epsilon_{\rm c}T_0/D_0^2$. For example, to solve the problem $\epsilon_{\rm c}T_0/D_0^2 = 10.0$, the solution for $\epsilon_{\rm c}T_0/D_0^2 = 5.0$ may be used as an initial solution to find the numerical solution for $\epsilon_{\rm c}T_0/D_0^2 = 5.50$. Subsequently, the solution for $\epsilon_{\rm c}T_0/D_0^2 = 5.50$ is used to obtain the solution for $\epsilon_{\rm c}T_0/D_0^2 = 6.0$. The value of $\epsilon_{\rm c}T_0/D_0^2$ is gradually increased by 0.5 until the final solution for $\epsilon_{\rm c}T_0/D_0^2 = 10.0$ is obtained. For smaller $\epsilon_{\rm c}T_0/D_0^2$, the required numerical solution may be obtained in three or four iterations. (In the iterative scheme, the convergence criterion used is that the values of $D^{(n)}(t)$ (at the collocation points on the crack) as calculated in (33) do not change by more than 0.5% in two consecutive iterations.) For $\epsilon_{\rm c}T_0/D_0^2 > 10$, $D^{(n)}(t)$ as calculated using (33) may converge very slowly or in an oscillatory manner. For larger $\epsilon_{\rm c}T_0/D_0^2$, the convergence of the solution may be improved significantly by modifying (33) for updating $D^{(n)}(t)$ as

$$\begin{aligned} D^{(n)}(t) &= -\omega\epsilon_{\rm c}\{\sum_{j=1}^{J}\psi_4^{(nj)}U^{(j-1)}(t)\}[\sum_{p=1}^{2}\sum_{j=1}^{J}\psi_p^{(nj)}U^{(j-1)}(t)m_p^{(n)}]^{-1} \\ &\quad +(1-\omega)D_{\rm last}^{(n)}(t) \end{aligned} \tag{45}$$

where $D_{\rm last}^{(n)}(t)$ is the approximation of $D^{(n)}(t)$ in the last iteration and ω is an appropriately chosen relaxation parameter. Using $\omega = 1/2$, we manage to obtain convergence for $D^{(n)}(t)$ for up to $\epsilon_{\rm c}T_0/D_0^2 = 50$. (The values of $K_{IV}(a,0)/(D_0\sqrt{a})$ in Table 1 for $\epsilon_{\rm c}T_0/D_0^2 = 20$ and $\epsilon_{\rm c}T_0/D_0^2 = 50$ are computed by using $\omega = 1/2$.) The numerical value of $K_{IV}(a,0)/(D_0\sqrt{a})$ in Table 1 for $\epsilon_{\rm c}T_0/D_0^2 \to \infty$ is obtained directly by using the numerical Green's function for permeable cracks as given in Athanasius, Ang and Sridhar [5].

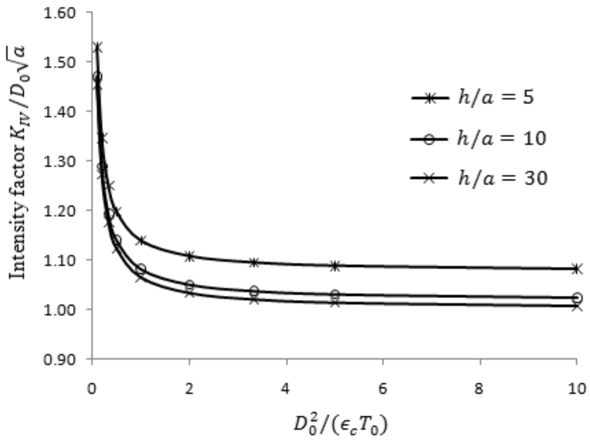

Figure 1. Plots of $K_{IV}(a,0)/(D_0\sqrt{a})$ against $D_0^2/(\epsilon_c T_0)$ for $h/a = 5$, 10 and 30.

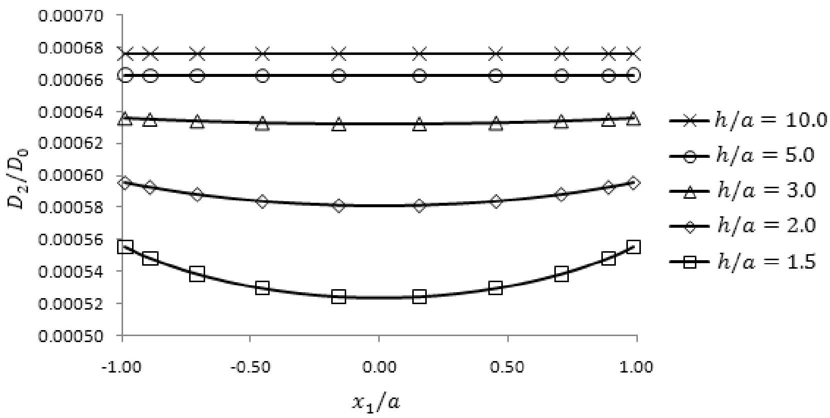

Figure 2. Plots of $D_2(x_1,0)/D_0$ against $-1 < x_1/a < 1$ for selected values of h/a with $\epsilon_c T_0/D_0^2 = 0.01$.

In Figure 1, $K_{IV}(a,0)/(D_0\sqrt{a})$ is plotted against $D_0^2/(\epsilon_c T_0)$ for $h/a = 5$, 10 and 30. For a fixed h/a, $K_{IV}(a,0)/(D_0\sqrt{a})$ decreases in magnitude and tends to a limiting value as $D_0^2/(\epsilon_c T_0)$ increases. Note the effects of the exterior boundary of the piezoelectric solid on $K_{IV}(a,0)/(D_0\sqrt{a})$. For a particular $D_0^2/(\epsilon_c T_0)$, when the boundary is closer to the crack, it appears that $K_{IV}(a,0)/(D_0\sqrt{a})$ has a higher magnitude.

In Figure 2, plots of $D_2(x_1,0)/D_0$ against $-1 < x_1/a < 1$ are given for $\epsilon_c T/D_0^2 = 0.01$ and selected values of h/a. For smaller values of h/a, it may be necessary to employ a larger number of boundary elements. For the numerical calculation to obtain the plots in Figure 2, up to 80 elements are employed on the exterior boundary. For larger values of h/a, such as $h/a = 5$ and $h/a = 10$, $D_2(x_1,0)/D_0$ is almost a constant over $-1 < x_1/a < 1$. This observation is consistent with the assumption of constant D_2 over the crack used in the derivation of the analytic solution for $h/a \to \infty$ (see Appendix). For smaller values of h/a, the variation of $D_2(x_1,0)/D_0$ over $-1 < x_1/a < 1$ is more prominent. The value of $D_2(x_1,0)/D_0$ is minimum at the center of the crack and increases towards the tips, as the field lines of D_2 perpendicular to the crack always tend to deviates towards the tips.

Figure 3 shows the variation of D_2/D_0 along the crack for $h/a = 30$ and selected values of $\epsilon_c T/D_0^2$. It can be seen that D_2/D_0 has a bigger magnitude for a higher value of $\epsilon_c T_0/D_0^2$. This is as expected because there is a lower resistance to the electrical conductance if the permittivity in the crack is higher.

Figure 4 gives plots of $D_0\Delta\phi(x_1,0)/(2hT_0)$ against $0 \leq x_1/a \leq 1$ for $h/a = 30$ and some selected values of $\epsilon_c T_0/D_0^2$. As may be expected, the value of $D_0\Delta\phi(x_1,0)/(2hT_0)$ at each point on the crack increases with decreasing $\epsilon_c T_0/D_0^2$.

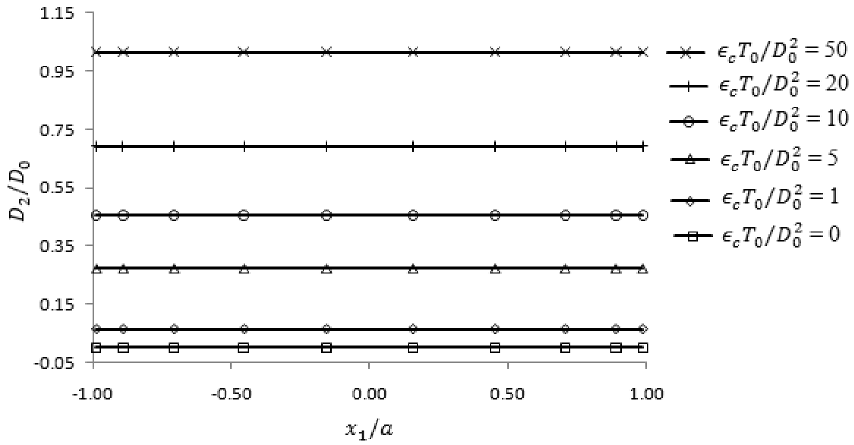

Figure 3. Plots of $D_2(x_1, 0)/D_0$ against $-1 < x_1/a < 1$ for selected values of $\epsilon_c T_0/D_0^2$ with $h/a = 30$.

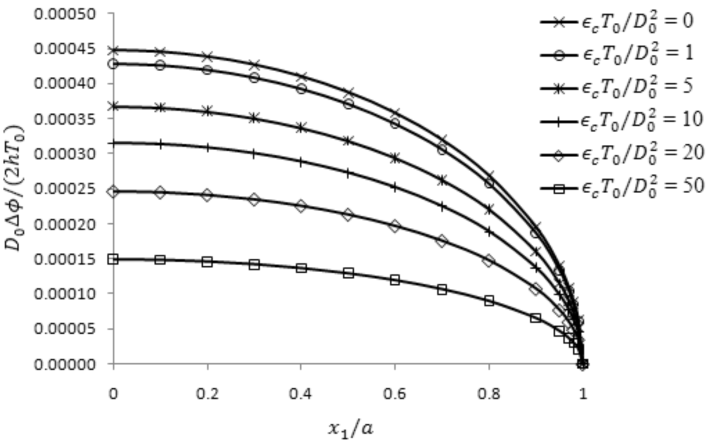

Figure 4. Plots of $D_0\Delta\phi(x_1, 0)/(2hT_0)$ against $0 \leq x_1/a \leq 1$ for some selected values of $\epsilon_c T_0/D_0^2$ with $h/a = 30$.

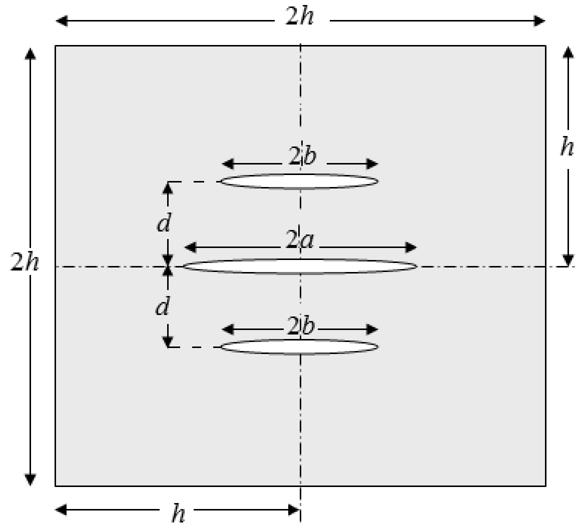

Figure 5. Three parallel cracks in a square domain.

For another problem, let us consider three parallel cracks $\gamma^{(1)}$, $\gamma^{(2)}$ and $\gamma^{(3)}$ in the domain $-h < x_1 < h$, $-h < x_2 < h$, where h is a given positive constant. The crack $\gamma^{(1)}$ lies in the region $-a < x_1 < a$, $x_2 = 0$, $\gamma^{(2)}$ in $-b < x_1 < b$, $x_2 = d$, and $\gamma^{(3)}$ in $-b < x_1 < b$, $x_2 = -d$, where a, b and d are given positive constants. Refer to Figure 5.

The boundary conditions on the sides of the square domain are given by

$$\left.\begin{array}{l} P_1 = \pm S_0 \\ P_2 = \pm T_0 \\ P_3 = 0 \\ P_4 = \pm D_0 \end{array}\right\} \text{for } -h < x_1 < h \text{ on } x_2 = \pm h,$$

$$\left.\begin{array}{l} P_1 = 0 \\ P_2 = \pm S_0 \\ P_3 = 0 \\ P_4 = 0 \end{array}\right\} \text{for } -h < x_2 < h \text{ on } x_1 = \pm h, \tag{46}$$

where S_0, T_0 and D_0 are given positive constants.

The constitutive relations are as before in (36) and (37). For the purpose of computation, the loads S_0, T_0 and D_0 are given the ratios $D_0/T_0 = 10^{-10}$ C/N and $D_0/S_0 = 10^{-10}$ C/N and the material constants in (44) are used.

For fixed $h/a = 30$ and $b/a = 1$, in Figures 6, 7 and 8, $K_I(a,0)/(T_0\sqrt{a})$, $K_{II}(a,0)/(S_0\sqrt{a})$ and $K_{IV}(a,0)/(D_0\sqrt{a})$ (at the tip $(a,0)$ of the center crack) are plotted against d/a for some values of $\epsilon_c T_0/D_0^2$ including $\epsilon_c T_0/D_0^2 = 0$ (impermeable cracks) and $\epsilon_c T_0/D_0^2 \to \infty$ (permeable cracks). The calculation for $\epsilon_c T_0/D_0^2 \to \infty$ is carried out using the numerical Green's function for permeable cracks in Athanasius, Ang and Sridhar [5].

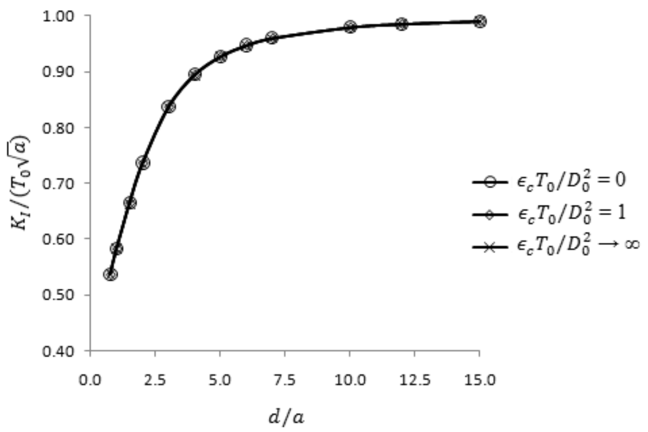

Figure 6. Plots of $K_I(a,0)/(T_0\sqrt{a})$ against d/a for $\epsilon_c T_0/D_0^2 = 0$, $\epsilon_c T_0/D_0^2 = 1$ and $\epsilon_c T_0/D_0^2 \to \infty$ with $h/a = 30$ and $b/a = 1$.

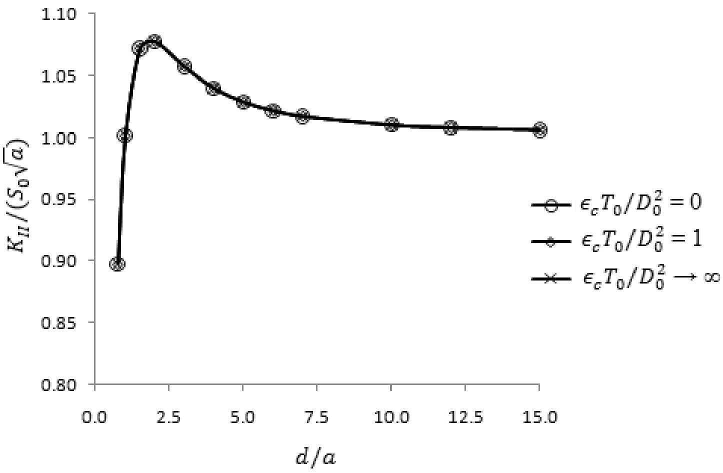

Figure 7. Plots of $K_{II}(a,0)/(S_0\sqrt{a})$ against d/a for $\epsilon_c T_0/D_0^2 = 0$, $\epsilon_c T_0/D_0^2 = 1$ and $\epsilon_c T_0/D_0^2 \to \infty$ with $h/a = 30$ and $b/a = 1$.

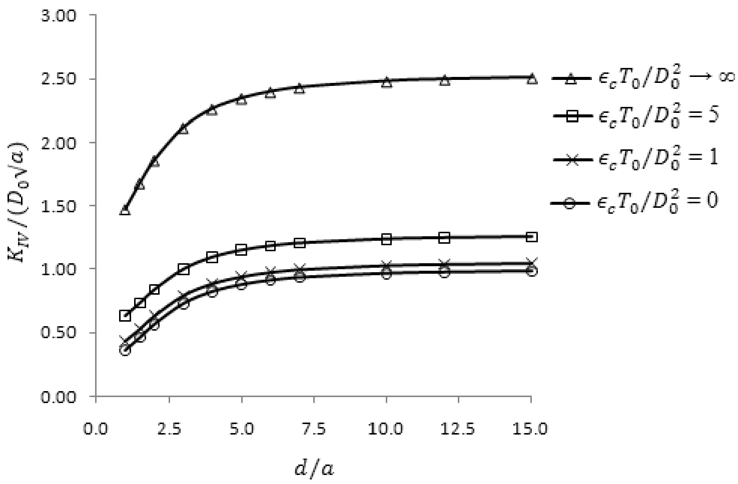

Figure 8. Plots of $K_{IV}(a,0)/(D_0\sqrt{a})$ against d/a for $\epsilon_c T_0/D_0^2 = 0$, $\epsilon_c T_0/D_0^2 = 1$, $\epsilon_c T_0/D_0^2 = 5$ and $\epsilon_c T_0/D_0^2 \to \infty$ with $h/a = 30$ and $b/a = 1$.

In Figure 6, the graphs of $K_I(a,0)/(T_0\sqrt{a})$ for $\epsilon_c T_0/D_0^2 = 0$, $\epsilon_c T_0/D_0^2 = 1$ and $\epsilon_c T_0/D_0^2 \to \infty$ are visually indistinguishable. Similarly, there is no distinction between the graphs of $K_{II}(a,0)/(S_0\sqrt{a})$ for $\epsilon_c T_0/D_0^2 = 0$, $\epsilon_c T_0/D_0^2 = 1$ and $\epsilon_c T_0/D_0^2 \to \infty$ in Figure 7. It appears that the permittivity of the medium filling the cracks has no significant effect on $K_I(a,0)/(T_0\sqrt{a})$ and $K_{II}(a,0)/(S_0\sqrt{a})$. In Figure 8, however, the magnitude of $K_{IV}(a,0)/(D_0\sqrt{a})$ appears to increase with $\epsilon_c T_0/D_0^2$. Note that the non-dimensionalized stress intensity factors $K_I(a,0)/(T_0\sqrt{a})$ and $K_{II}(a,0)/(S_0\sqrt{a})$ in Figures 6 and 7 are close to unity for large d/a. This is as expected since $K_I(a,0)/(T_0\sqrt{a})$ and $K_{II}(a,0)/(S_0\sqrt{a})$ should both be unity for the corresponding case of a single crack in an infinite piezoelectric space.

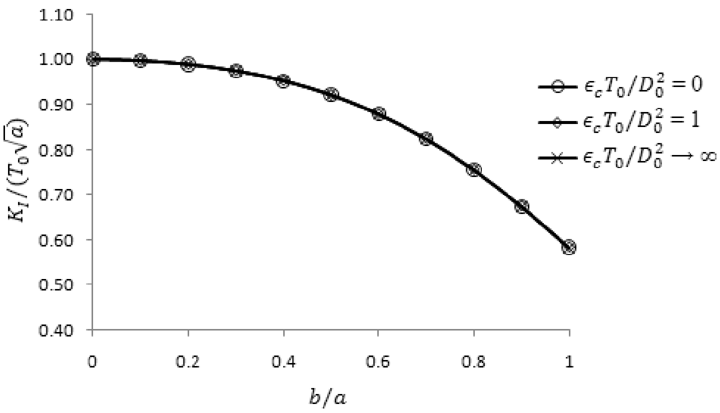

Figure 9. Plots of $K_I(a,0)/(T_0\sqrt{a})$ against b/a for $\epsilon_c T_0/D_0^2 = 0$, $\epsilon_c T_0/D_0^2 = 1$ and $\epsilon_c T_0/D_0^2 \to \infty$ with $h/a = 30$ and $d/a = 1$.

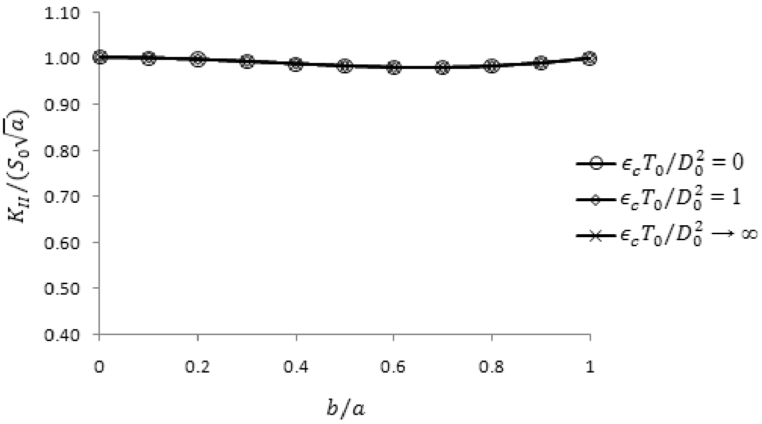

Figure 10. Plots of $K_{II}(a,0)/(S_0\sqrt{a})$ against b/a for $\epsilon_c T_0/D_0^2 = 0$, $\epsilon_c T_0/D_0^2 = 1$ and $\epsilon_c T_0/D_0^2 \to \infty$ with $h/a = 30$ and $d/a = 1$.

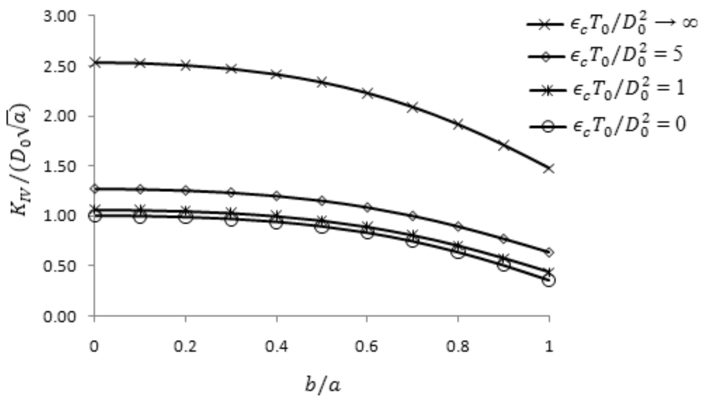

Figure 11. Plots of $K_{IV}(a,0)/(D_0\sqrt{a})$ against b/a for $\epsilon_c T_0/D_0^2 = 0$, $\epsilon_c T_0/D_0^2 = 1$, $\epsilon_c T_0/D_0^2 = 5$ and $\epsilon_c T_0/D_0^2 \to \infty$ with $h/a = 30$ and $d/a = 1$.

For fixed $h/a = 30$ and $d/a = 1$, Figures 9, 10 and 11 show the plots of $K_I(a,0)/(T_0\sqrt{a})$, $K_{II}(a,0)/(S_0\sqrt{a})$ and $K_{IV}(a,0)/(D_0\sqrt{a})$ against b/a $(0 \leq b/a \leq 1)$ for various values of $\epsilon_c T_0/D_0^2$. As in Figures 6 and 7,

$K_I(a,0)/(T_0\sqrt{a})$ and $K_{II}(a,0)/(S_0\sqrt{a})$ for $\epsilon_c T_0/D_0^2 \to \infty$ in Figures 9 and 10 are not distinguishable from the corresponding non-dimensionalized intensity factors for $\epsilon_c T_0/D_0^2 = 0$ and $\epsilon_c T_0/D_0^2 = 1$. For very small b/a, $K_I(a,0)/(T_0\sqrt{a})$ and $K_{II}(a,0)/(S_0\sqrt{a})$ are close to one. This is consistent with the observation in Figures 6 and 7 that the non-dimensionalized intensity factors are close to one for larger d/a.

For fixed $\epsilon_c T_0/D_0^2 = 1$, $h/a = 30$ and $d/a = 1$, Figure 12 shows the variation of D_2/D_0 along the center crack and various values of the crack length ratio b/a. It appears that as b/a increases the non-dimensionalized normal electrical displacement D_2/D_0 becomes larger in magnitude and exhibits a greater variation over the center crack.

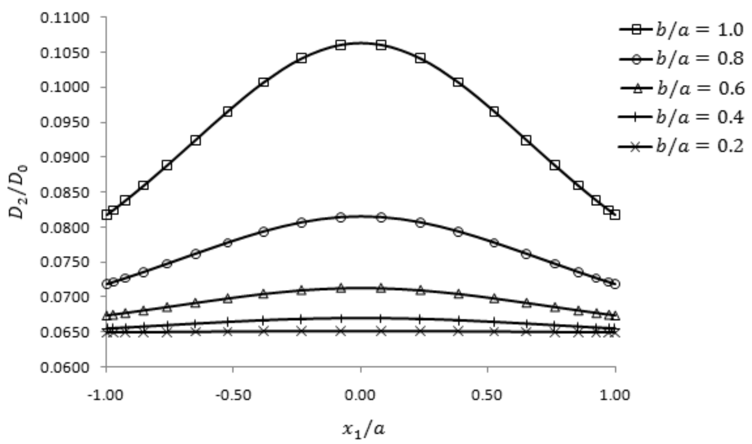

Figure 12. Plots of $D_2(x_1,0)/D_0$ against x_1/a for various values of b/a with $\epsilon_c T_0/D_0^2 = 1$, $h/a = 30$ and $d/a = 1$.

8 Summary

An iterative method based on the electro-elastostatic boundary integral equations together with the numerical Green's function for impermeable cracks (as derived in Athanasius, Ang and Sridhar [5]) has been successfully implemented for the analysis of electrically semi-permeable cracks in a piezoelectric solid. As the conditions on the semi-permeable cracks are not fully satisfied by the Green's function (for impermeable cracks), the resulting boundary integral formulation involves integrals whose integrands are given by a non-linear function of the crack opening displacement and the electrical potential jump on the cracks. Nevertheless, if the crack opening displacement and the electric potential jump are assumed known, a simple boundary element procedure which involves only unknowns on the exterior boundary of the piezoelectric solid can be devised. The approach proposed here for the numerical solution of the electroelastic crack problem is to iterate to and fro estimating the crack opening displacement and the electrical potential jump and using the simple boundary element procedure to determine the unknowns on the exterior boundary.

For a particular problem involving a single planar crack which is centrally located in a very large piezoelecric plate under uniform loads, the numerical values obtained for the crack tip stress and electric displacement intensity factors are found to be in good agreement with those computed using analytical formulae. Qualitatively acceptable results are also obtained for some specific problems including one which involves the interaction of three parallel planar cracks.

References

[1] M Abramowitz and IA Stegun, *Handbook of Mathematical Functions*, Dover, New York, 1971.

[2] WT Ang, A boundary integral equation for deformations of an elastic body with an arc crack, *Quarterly of Applied Mathematics* **45** (1987) 131-139.

[3] WT Ang and DL Clements, A boundary element method for determining the effect of holes on the stress distribution around a crack, *International Journal for Numerical Methods in Engineering* **23** (1986) 1727-1737.

[4] WT Ang and JCF Telles, A numerical Green's function for multiple cracks in anisotropic bodies, *Journal of Engineering Mathematics* **49** (2004) 197-207.

[5] L Athanasius, WT Ang and I Sridhar, Numerical Green's functions for some electroelastic crack problems, *Engineering Analysis with Boundary Elements* **33** (2009) 778-788.

[6] DM Barnett and J Lothe, Dislocations and line charges in anisotropic piezoelectric insulators, *Physica Status Solidi (b)* **67** (1975) 105-111.

[7] DL Clements, *Boundary Value Problems Governed by Second Order Elliptic Systems*, Pitman, London, 1981.

[8] DL Clements and MD Haselgrove, A boundary integral equation method for a class of crack problems in anisotropic elasticity, *International Journal of Computer Mathematics* **12** (1983) 267-278.

[9] M Denda, BEM analysis of semipermeable piezoelectric cracks, *Key Engineering Materials* **383** (2008), 67-84.

[10] HJ Ding, GQ Wang and WQ Chen, A boundary integral formulation and 2D fundamental solutions for piezoelectric media, *Computer Methods in Applied Mechanics and Engineering* **158** (1998) 65-80.

[11] GF Gao and WX Fan, The fundamental solutions for the plane problem in piezoelectric media with an elliptic hole or a crack, *Applied Mathematics and Mechanics* **19** (1998) 1043-1052.

[12] F Garcia-Sanchez, SB Saez and J Dominguez, Anisotropic and piezoelectric materials fracture analysis by BEM, *Computers & Structures* **83** (2005) 804-820.

[13] U Groh and M Kuna, Efficient boundary element analysis of cracks in 2D piezoelectric structures, *International Journal of Solids and Structures* **42** (2005) 2399-2416.

[14] T H Hao and Z Y Shen, A new electric condition of electric fracture mechanics and its applications, *Engineering Fracture Mechanics* **47** (1994) 793-802.

[15] S Guimarães and JCF Telles, General application of numerical Green's functions for SIF computations with boundary elements, *Computer Modeling in Engineering and Sciences* **1** (2000) 131-139.

[16] E Pan, A BEM analysis of fracture mechanics in 2D anisotropic piezoelectric solids, *Engineering Analysis with Boundary Elements* **23** (1999) 67-76.

[17] RKND Rajapakse and XL Xu, Boundary element modeling of cracks in piezoelectric solids, *Engineering Analysis with Boundary Elements* **25** (2001) 771-781.

[18] JCF Telles, GS Castor and S Guimarães, A numerical Green's function approach for boundary elements applied to fracture mechanics, *International Journal for Numerical Methods in Engineering* **38** (1995) 3259-3274.

[19] XL Xu and RKND Rajapakse, Boundary element analysis of piezoelectric solids with defects, *Composites Part B: Engineering* **29** (1998) 655-669.

[20] MD Snyder and TA Cruse, Boundary integral analysis of cracked anisotropic plates, *International Journal of Fracture* **11** (1975) 315-328.

Appendix

An analytic solution to the problem of a semi-permeable crack in an infinite piezoelectric medium is given here. The crack lies in the region $-a < x_1 < a$, $x_2 = 0$.

For the solution of the problem, let the generalized stress be given by

$$S_{Kj} = S_{Kj}^{(0)} + S_{Kj}^{(1)}, \tag{A1}$$

where $S_{Kj}^{(0)}$ are the constants giving the uniform state of the generalized stress in the absence of the crack and $S_{Kj}^{(1)}$ are induced by the crack such that $S_{K2}^{(0)} + S_{K2}^{(1)} = 0$ on the crack for $K = 1$, 2 and 3.

The induced generalized stress $S_{Kj}^{(1)}$ and its corresponding generalized displacement $U_K^{(1)}$ are given by

$$\begin{aligned} U_K^{(1)} &= \mathrm{Re}\{\sum_{\alpha=1}^{4} A_{K\alpha} M_{\alpha S} P_S[-z_\alpha + (z_\alpha^2 - a^2)^{1/2}]\}, \\ S_{Kj}^{(1)} &= \mathrm{Re}\{\sum_{\alpha=1}^{4} L_{Kj\alpha} M_{\alpha S} P_S[-1 + \frac{z_\alpha}{(z_\alpha^2 - a^2)^{1/2}}]\}, \end{aligned} \qquad \text{(A2)}$$

where $P_1 = S_{12}^{(0)}$, $P_2 = S_{22}^{(0)}$, $P_3 = S_{32}^{(0)}$ and, as in Hao and Shen [14], P_4 is assumed to be a constant yet to be determined and $(z_\alpha^2 - a^2)^{1/2}$ is defined in such a way that

$$\lim_{|z_\alpha| \to \infty} \frac{z_\alpha}{(z_\alpha^2 - a^2)^{1/2}} = 1. \qquad \text{(A3)}$$

It is easy to check that $S_{K2}^{(1)} = -P_K$ on the crack. Thus, $S_{Kj}^{(1)}$ satisfies the traction free conditions on the crack, that is, $S_{K2}^{(0)} + S_{K2}^{(1)} = 0$ on the crack for $K = 1$, 2 and 3, as required. Furthermore, it can be shown that $S_{Kj}^{(1)} \to 0$ as $|z_\alpha| \to \infty$, that is, the generalized stress is given by $S_{Kj}^{(0)}$ at infinity.

The crack is electrically semi-permeable, that is,

$$S_{42} \Delta U_2 = -\epsilon_c \Delta U_4 \text{ on the crack.} \qquad \text{(A4)}$$

From (A1) and (A2), $S_{42} = S_{42}^{(0)} - P_4$ on the crack, and if P_4 is to be a real, then

$$\Delta U_2 = \mathrm{Re}\{\sum_{\alpha=1}^{4} 2i A_{2\alpha} M_{\alpha S}\} P_S (a^2 - x_1^2)^{1/2} \text{ for } -a < x_1 < a. \qquad \text{(A5)}$$

It follows that (A4) is satisfied if

$$(S_{42}^{(0)} - P_4) V_{2S} P_S = -\epsilon_c V_{4S} P_S, \qquad \text{(A6)}$$

where

$$V_{KS} = \mathrm{Re}\{\sum_{\alpha=1}^{4} 2iA_{K\alpha}M_{\alpha S}\}. \tag{A7}$$

Note that (A6) is a quadratic equation in the unknown parameter P_4. If a unique constant P_4 satisfying (A6) and the inequality $V_{2S}P_S > 0$ (so that $\Delta U_2 > 0$) can be found, we have obtained an analytic solution to the problem of the single semi-permeable crack. The value of P_4 for the special case of an electrically impermeable crack ($\varepsilon_\mathrm{c} = 0$) or a permeable crack ($\varepsilon_\mathrm{c} \to \infty$) can be easily obtained from (A6). Specifically,

$$P_4 = \begin{cases} S_{42}^{(0)} \text{ for an impermeable crack,} \\ -V_{44}^{-1} \sum\limits_{k=1}^{3} V_{4k}P_k \text{ for a permeable crack.} \end{cases} \tag{A8}$$

Once P_4 is determined, the crack tip stress and electric displacement intensity factors can be easily extracted from (A2).